



# Classification of Alzheimer's disease Using DBN, SVM and Random Forest Models

M.Rajendiran<sup>1</sup>, Dr.K.P. Sanal Kumar<sup>2</sup>, Dr.S.Anu H Nair<sup>3</sup>

<sup>1</sup>Research Scholar, Department of Computer and Information Sciences, Annamalai University, Chidambaram, India

<sup>2</sup>Assistant Professor, PG Department of Computer Science, R. V. Government Arts College, Chengalpattu, India

<sup>3</sup>Assistant Professor, Department of CSE, Annamalai University, Chidambaram, India (Deputed to WPT, Chennai)

<sup>1</sup>rajendiran\_m@yahoo.com, <sup>2</sup>sanalprabha@yahoo.co.in, <sup>3</sup>anu\_jul@yahoo.co.in

## ABSTRACT

In Alzheimer's disease detection, the early detection of morphological differences is challenging to provide pre-treatment. MRI imaging technique is utilised to detect the severity level of AD in patients. Hence, by analysing hippocampus volume using magnetic resonance imaging (MRI), the AD disease level can detect. Measuring hippocampus volume requires a great deal of time and is not feasible for manual segmentation [1]. Automatic segmentation is required to bypass these restrictions and obtain the AD biomarkers. MRI is widely preferred for obtaining detailed structural brain images in three dimensions (3-D). In this imaging technique, vivo voxel dimensions of certain structures influenced by disease progressions can be obtained. Structural MRI is broadly accessible, provides better accuracy of diagnosis and has reasonable costs.

Furthermore, MRIs indicate higher associations with the progression of mild cognitive impairments (MCI) to AD. However, the dissimilarities between progressive MCI (pMCI) and stable MCI (sMCI) are too minute to be discovered via MRI. This refined dissimilarity has emerged from huge inter subject inconsistencies and age-linked deviations. Hence, predicting MCI-to-AD conversion by MRI scanning is an arduous task. In the current comprehensive literature, the particle swarm optimisation-based fuzzy c-means technique has been appraised for segmenting the brain region. This process utilised a limited number of validation parameters to validate the segmentation accuracy.

**Keywords:** Alzheimer, Detection, Classification, Histogram Normalization.

**DOI Number:**10.14704/nq.2022.20.8.NQ44538

**NeuroQuantology 2022; 20(8): 5117-5132**

## INTRODUCTION

Consequently, it needs develop more innovative approaches for detecting MCI-to-AD conversion. Accurate segmentation of the hippocampus region via 3-D MR imaging requires eminent expertise to represent the organisation of each MRI slice manually. In many diagnoses, especially that of AD, volumes on a single MR image are not enough. It also must to measure the changes

over time. Change data can rule out several vital biological discrepancies and help monitor the progression of the disease. The large inter subject variability can decrease with the help of spatial registration on a mutual plot for evaluation. Various registration methods have been presented in the literature for sorting anatomies at various levels. Affine registration utilised and some other perfect non-rigid registrations were exploited. Via precise



registration techniques, they effectively arranged anatomical formations of various matters for assessment, learning that the disease varies between subjects may be relatively detached. However, when the registration process did not implement, inter-subject uncertainty and disease deviations among subjects were well-maintained [2]. Still, if the inter-subject variability increases, the perceptive pathological disparities may be veiled, and the classification analysis of MCI controls could burden.

In some instances where the registration process is nearly perfect, inter-subject uncertainty and morphological difference are eliminated. Because the boundaries of the hippocampus region obtained from MRI scans are imperfect, knowledge of primary data is essential for obtaining accurate markers. Primary data can be obtained using the statistical information of shape deformations or using the registration process with a single object atlas template. The automatic segmentation of GM, WM, CSF and Hippocampus requires receiving an accurate brain tumour volume. Measuring the volume of these segments does not provide efficiency in manual segmentation. Automatic segmentation analysis requires eliminating the restriction, as mentioned

earlier. In the previous chapter, accurate segmentation is achieved with updated techniques. The combinational of K -means clustering and graph-cut methods are proposed to enhance the segmentation and classification performances. In classification analysis, the cluster region is assigned the labels based on its features. In this analysis, we have classified various Alzheimer's' disease stages such as the initial stage, middle stage, and final stage.

#### **OBJECTIVES**

- Intensity normalisation is used to compare various images in the training set.
- To enhance the segmentation technique, the K -means clustering method is used with graph-cut methods.
- Finally, game theory is used to improve the performance of Alzheimer's disease classification.

#### **2. PROPOSED MODEL**

In the proposed system, the various stages involved to extract efficient features and classification analysis. The GLCM features are selected to attain the classification. Figure 1 describes the overall flow of the proposed method.



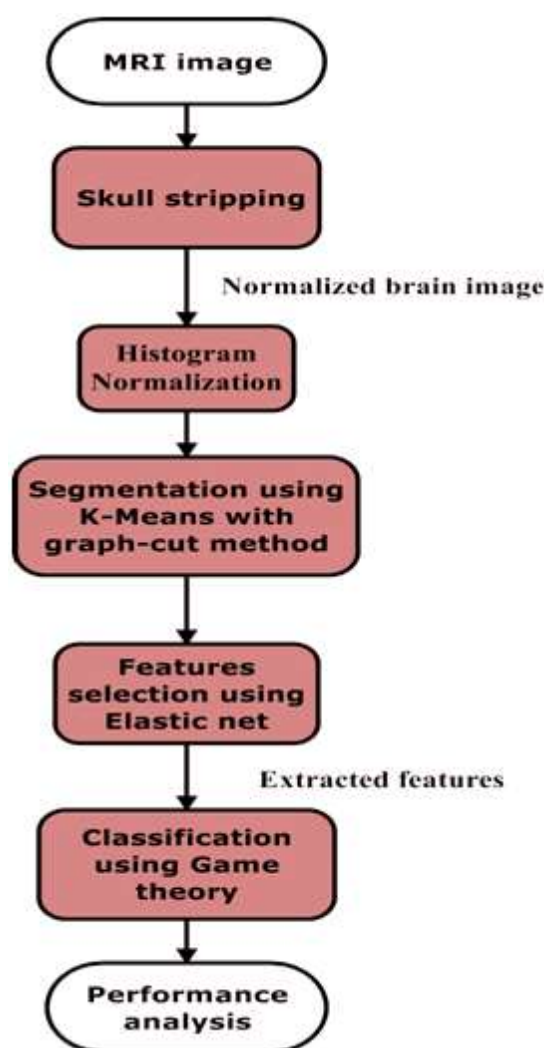


*Figure 1 Work flow of the proposed system*

## 2.1. REGISTRATION AND INTENSITY NORMALISATION

Image registration defines the arrangement of two images for comparison, and it makes easily visible. In this registration process, the two images are taken at various viewpoints, various times, and various imaging techniques. These images are aligned geometrically, which determines a geometric transformation of those two images. The geometric transformation is involved using mapping functions.

In this work, the image registration process will be performed, and the pathological variations are carried out. After the precious registration, the template images are obtained and determined the intensities among subjects normalised. The selected input image of the histogram is attained and then distorted to equal the histogram [3].

Generally, a histogram defined as the graphical representation of pixel intensity value in the image. This process enhances the image contrast that adjusts the Greyscale range of the image. In the OASIS database, the histogram of MNI52 images is received as a basic histogram. When image registration and histogram normalisation, the chosen images are arranged to specific template areas that match the intensity values. In the end, the features are used for training and testing purposes. So, the input images and template of normal intensities are selected as features.

In the histogram technique, the minimum intensity regions of histograms define to cut off and background voxel of the image. Therefore, intensity can choose and view on an advanced scale. Various images of histograms appear in location and shape, and

they had the same intensity distribution after normalisation. The histogram normalisation modifies the intensities to receive the highest contrast.

Input image defined as  $G$ , in matrix form an image  $xb$ , pixel values ranges from  $[0,$

$$H_n = \frac{\text{number of pixels with the pixel value of } V}{\text{Total number of pixels}} \quad (1)$$

$(V - 1)]$ .  $V$  defines the number of pixel values.  $H_n$  defines the normalised histogram value of  $G$  for each pixel value (refers to equation (1)).

Where  $V = 0, 1, \dots (V - 1)$

The histogram of normalized image is calculated (refers to equation (2)).

$$H_{i,j} = \text{floor} \left[ \left( (V - 1) \sum_{v=0}^{G_{i,j}} H_n \right) \right] \quad (2)$$

The floor ( $\cdot$ ) function is utilized to analyse the closest integer value. The transformation of pixel used in below function (refers to equation (3)).

$$T(p) = \text{floor} \left[ \left( (V - 1) \sum_{v=0}^p H_n \right) \right] \quad (3)$$

In this transformation,  $G$  and  $H$  measured as continuous random variables  $X$  and  $Y$  on  $[0, (V - 1)]$  using (refers to equation (4)).

$$X = T(Y) = (L - 1) \int_0^y p_Y(y) dy \quad (4)$$

0

$P_Y \rightarrow$  probability density function (PDF)

" $T$ "  $\rightarrow$  cumulative distributive function  $[0, V-1]$ ,

Distributed function  $P_Y = \frac{1}{p-1}$  denoted (refers to equation (5)).

$(z) dz = \text{PDF that } 0 \leq Y \leq y = \text{PDF (5)}$

that  $0 \leq X \leq T^{-1}(x)$  (6)

$$\frac{d}{dx} \left( \int_0^x P_Y(Z) \right) = 1_Y(y) = P_X(T^{-1}y) \frac{d}{dy} (T^{-1}(y)) \quad (7)$$

The weighting of the histogram is measured with the help of Distributed function.  $P_X(x)$  and  $P_Y(y)$  are the grey-level PDFs of the input and output images with grey-level intensities  $x$  and  $y$ , respectively (refers to equation (6)).

$P_Y(Z)$  is uniform Distributed function. Hence, the transformation above achieves the desired result, i.e., histogram of input image is

transformed to a target histogram which is calculated using (refers to equation (7)).

### SKULL STRIPPING

The skull stripping process extracts the brain from a large dataset accurately. Effective volume analysis and segmentation require removing the skull from an input image. It helps to analyse the accurate brain



in an MRI image. In this work, the skull stripping involves three operations: thresholding, removing narrow connections, and post-processing. Initially, the threshold value selection is the most important to create a mask for brain tissues. The threshold mask contains two conditions.

- The non-brain parts should be weak in brain connection.
- The mask should be safeguarded by more brain parts due to the high possibility to cut the mask in a special connection.

### REMOVING OF NORMAL AGEING EFFECTS

The classification of normal brain ageing is essential in the earlier stage of AD. The voxel-wise intensities of MC are used to calculate the normal ageing effects at every location with a linear regression model [6]. Here, "M" represents the healthy controls, and each healthy subject of an image contains N pixel volume. The normalised intensities are described with MC subjects as  $YT = (YT; YT; \dots YT' \dots YT) \in RM \times N$ . In this matrix, each row is described as  $y_i = [y_{i1}; y_{i2}; \dots \dots y_{iM}] \in R^1 \times M$ ;  $i = 1, 2, \dots N$ . A vector describes the M healthy patients of ages,  $V \in RM \times N$ . The age-related effects are measured using linear regression model  $y_{i1} = wiv + bi$  at every voxel independently. Then the effects of normal ageing will eliminate at the  $j$ th image of the  $i$ th voxel as  $Y_{new} = y_{ij} - wiaj - bi$ .

### FEATURE SELECTION

In the MRI image, there are a large number of voxels presented after the pre-processing process. The voxel does not contain information on pathological variations

$$E = \sum_{i=1}^k \sum_{x_i \in p_j} \|X_i - S_j\|^2 \quad (8)$$

In this (refers to equation (8)).  $X_i$  represents an  $i$ th pixel,  $S_j$  is the cluster center, and  $p_j$  represents the total no of clusters. K-means clustering algorithm selects k-point collective If  $Y_q$  belongs to  $P_j(m)$ ,  $Y_q \in P_j(m)$ , then

$$\|Y_q - P_j(m)\| < \|Y_q - P_i(m)\| \text{ for } i = 1, 2, 3 \dots k \text{ and } i \neq j \quad (9)$$

integrated into AD [7]. The essential features are selected using the GLCM matrix that represents the spatial relationship of image and distance. The GLCM matrix added the columns and rows that equal the sum of various greylevels of the subset. The ROI region of intensity variation is calculated with the GLCM elements. Two parameters are required to form the GLCM matrix, such as the distance of two pixels and the relative angle of two pixels. In the matrix,  $i^{th}$  and  $j^{th}$  element are described as  $g(i, j)$  that provides the relative frequency of the  $i^{th}$  and  $j^{th}$  element in the ROI region [8]. The angle is calculated between the angel in four directions 00, 900, 45 °, and 135 °. The GLCM features are correlation, contrast, variance, difference entropy, correlation measures, and correlation coefficient.

### Segmentation using K Means with graph-cut

In this work, the image segmentation involved a hybrid clustering method that combines k-means clustering and graph cut theory. The clustering approach performs the partitioning of the given dataset into multiple clusters [9]. In a single cluster, various pixels consist of the same pattern. K-means clustering method is an unsupervised learning technique that solves the clustering problem. In each iteration, the k-means reduces the sum of the distance from its clusters of each data. It had the advantage of clustering a huge amount of data, very popular, efficiently and quickly. K-means can easily determine the cluster centers, and it creates a certain number of non-hierarchical clusters. It measures the Euclidean distance among each pixel and its specific cluster centers.

vectors as the centre between n data vectors. Then the  $(n - k)$  remaining data distributed to their nearest cluster center (refers to equation (9)).



Total pixels are assigned to clusters, and again calculate the cluster center with the help of current membership. Then repeat the process until the measurement function starts to assemble. A multispectral image is described with the pair of  $(k, l)$ , and the existing finite discrete function is  $F(z > 0)$ .

The multispectral image will transport into a non-negative edge-weighted graph  $G(V, E)$ . In this graph,  $V$  represents the vertices in the image pixel, and  $E$  represents the edges between the pixels. The relation and deviation between the pixels exist based on the ratio of edges. The image is plotted into the network based on these representations, which

produce the network cutting rate. This rate is equal to the visual issues of the energy function.

In a directed graph, the vertices are defined as  $t \in \{1, 2, 3 \dots d\}$ ,  $t$ , whered represents the total no of the label. Consider  $M$  to be the number of vertices. In image  $G$  each vector defines  $t = \{t_1, t_2, t_3 \dots t_n\}$ . The energy function is estimated to allocate the label to every pixel. The energy segmentation is calculated by reducing the energy. The energy function works based on the Potts model, which contains two limitations: smooth constraint and data constraint (refers to equation (10)).

$$E(t) = E_{di}(t) + E_{smooth}(t) = \sum_y \in d_y P_y(t_y) + \sum_{x,y \in M} P_{x,y}(t_x, t_y) \quad (10)$$

Here,  $E_{di}(t)$  defines the penalty term,  $E_{smooth}(t)$  represents discontinuity penalty term and  $M$  defines the linking pairs of pixels,  $t_y$  defines the possibility of function.  $P_{x,y}(t_x, t_y)$  describes the PDF - Probability Density Function which provides similarity between  $x$  and  $y$ .

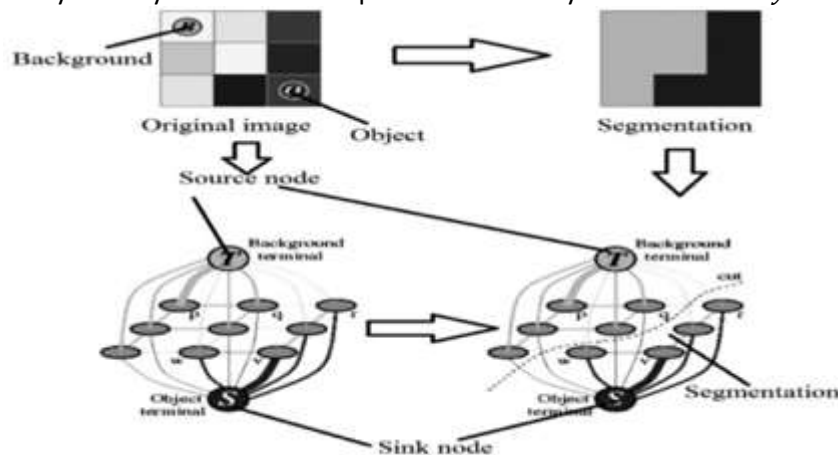


**Figure 2 Representation of K-means with graph cut algorithm**

Figure 2 represents the proposed K- Means with graph-cut algorithm. In this technique, the energy function is minimised and the data term is measured using the colour likelihood of background and foreground and spatial coherency. In the image, the boundary length is modulated with the difference by the latter term. So, it minimises the energy with a bias for smaller boundaries. This function is called "shrinking bias". Furthermore, it is a challenging task to segment the thin lengthened structures for the graph cut method [8]. The proposed method segments the exciting objects with lengthened and

delicate parts. The graph cut method achieves fast segmentation. It generates the graph for the image, where weighted edges connect each pixel.

This research work is developed to implement a different method of clustering information. Graph segregation is one of the clustering types that allocate  $G = (V, E)$ .  $A = |V| \times |V|$  represents the similarity matrix whose completion represents its corresponding edge weights to all connected vertices. When the similarity matrix  $A=0$ , that will not contain any edges between corresponding vertices [9].

The addition of edge weights can calculate the connection between vertices  $(A, B)$ . It can be defined as a mathematical form  $(A, B) = \sum n A_{ij}$ .

Furthermore, the degree of all vertices defined as  $D = \text{links}(A, V)$ . Graph separation defines the partitioning of the graph into  $k$  clusters or disconnected partitions  $V_1, \dots, V_k$ . Various strategies of cluster initialisation perform the segmentation process in the graph-cut and k-means approach.

### CLASSIFICATION USING GAME THEORY

The classification works in supervised learning, where the object is to predict the class label for unlabelled input instances. In this classification, the feature values are described from feature space [122]. The classification detection achieves based on the extracted knowledge from a sample of labelled instances. In the proposed work, the game theory is used for efficient classification. It includes a large number of decision-makers and the participators considered as players.

Moreover, Players consist of an array of individual moves in each game. Each player contains many opportunities in every move. These opportunities are selected from various existing possibilities. At the end of the game, players attain a specific payoff based on the played game of manner.

The game is represented as "G" within a group of players. The agent is described as set  $A = \{1, 2, \dots, a\}$ . In each player "i", the set of actions is denoted as  $\alpha_i$  and strategies  $S_i$ . Additionally, the individual payoff is denoted as  $P_i$  as a cost function represented as  $J_i$ . In every game, the participants or players select an optimal action independently to optimise their objective function to generate decisions. "S" specified as an object which is represented by a triplet  $(A, S, \alpha, J)$ .

Strategy space  $S = S_1 \times S_2 \times \dots \times S_m$

Actionspace  $\alpha = \alpha_1 \times \alpha_2 \times \dots \times \alpha_m$   $J: \alpha \in R^m$  stated as,

$$J(u) = [J_1(u), \dots, J_m(u)]^T, u \in \alpha \quad (11)$$

The objective function vector defines each player set  $N$ . Here,  $J$  represents the vector of the cost function (refers to equation (11)). It increases the vector of the payoff function. Consider every player involves to reduce costs. In the "One shot games" strategy, one argument is provided [123]. When the action  $\alpha_i$  represents the accessible actions to the "i" player, the finite or non-finite games should generate.

Algorithmic steps of Game theory:

Step 1: A heuristic payoff matrix is given as input. Step 2: Choose a random vector.

Step 3: Numerical integrate using initial conditions and payoffs. Step 4: Record the state vector which can be plotted in the simplex.

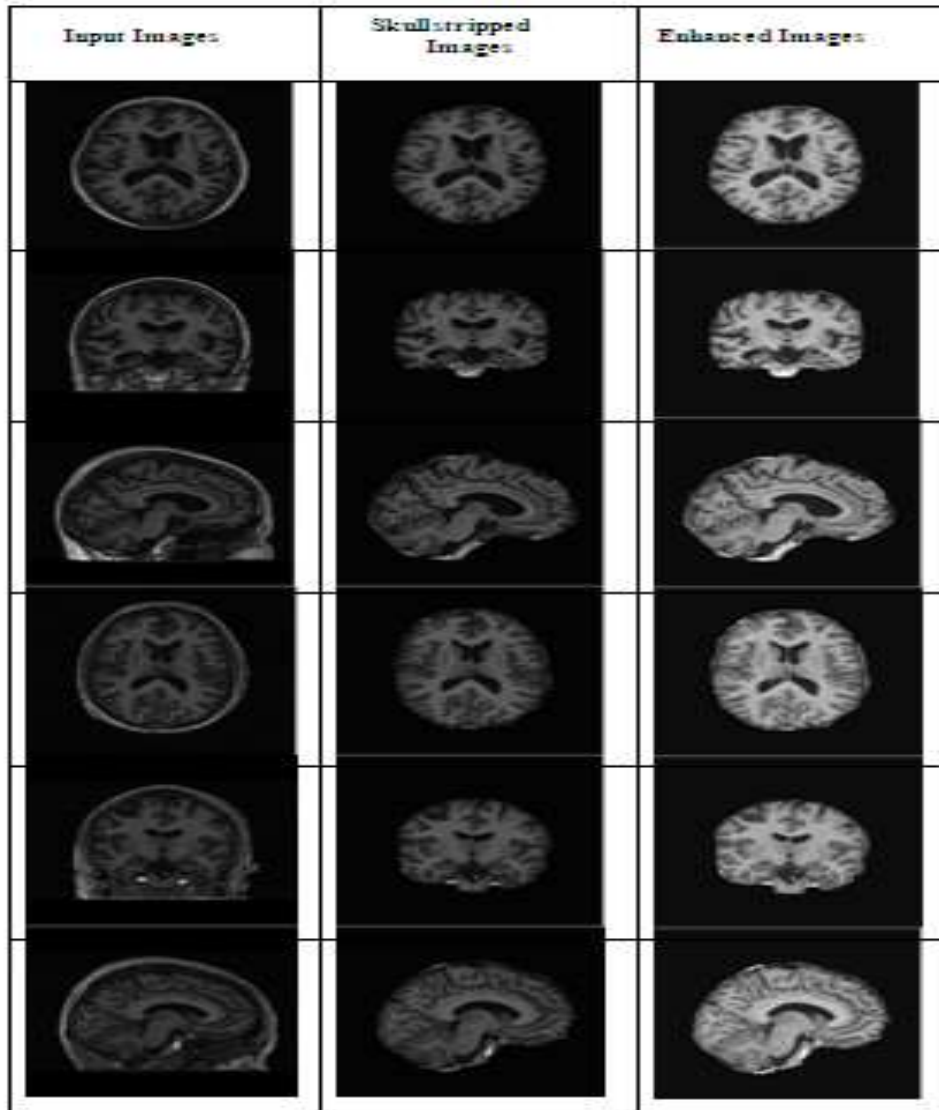
Step 5: Matching the state vectors according the Records in the game. Step 6: Decision making based upon the state vector matching.

The principle is analogous to the Shapley value, with an extended expression. Here, the underlying intuition is to reward a feature pair if they both contribute equally and produce good results, and to penalize a feature pair if it behaves asymmetrically (i.e. one agent consistently contributing more than the other), or if the pair tends not to improve coalitions it takes part. This research work treat GB model as the game setting, the model's features as our players, Area Under the Curve (AUC) as its characteristic function, and the predicted output of GB model as the common interest. The common interest here is the classification of AD or NC from a series of medication use observations. Features are evaluated in permutations by evaluating their expected output, and the best coalition of features, which produces the highest contribution to the common interest. The Classes have been assigned in four ways to classify the severity of AD which are NC vs pMCI, pMCI vs sMCI, sMCI vs AD with respect to the features.

### RESULTS AND DISCUSSION

The results section contains the output of the proposed technique and various performance measures of the proposed method to analyse the efficiencies.

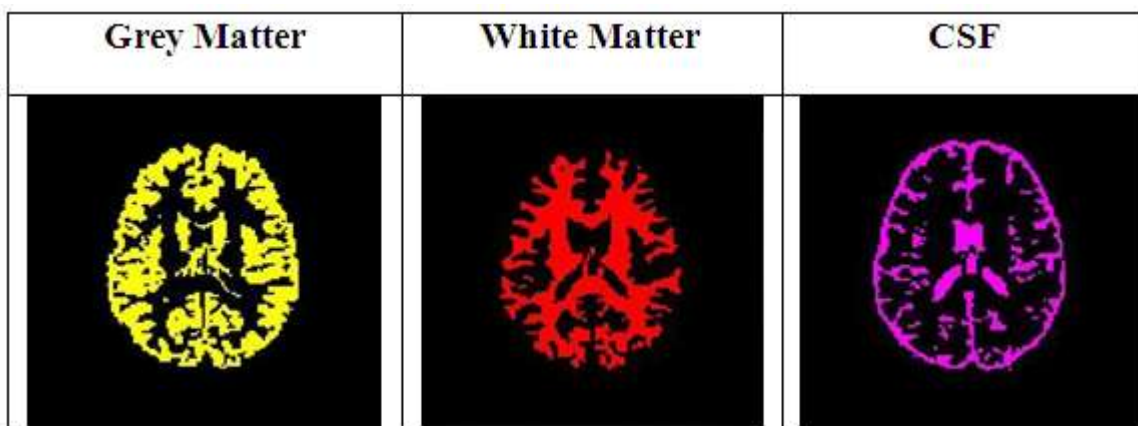




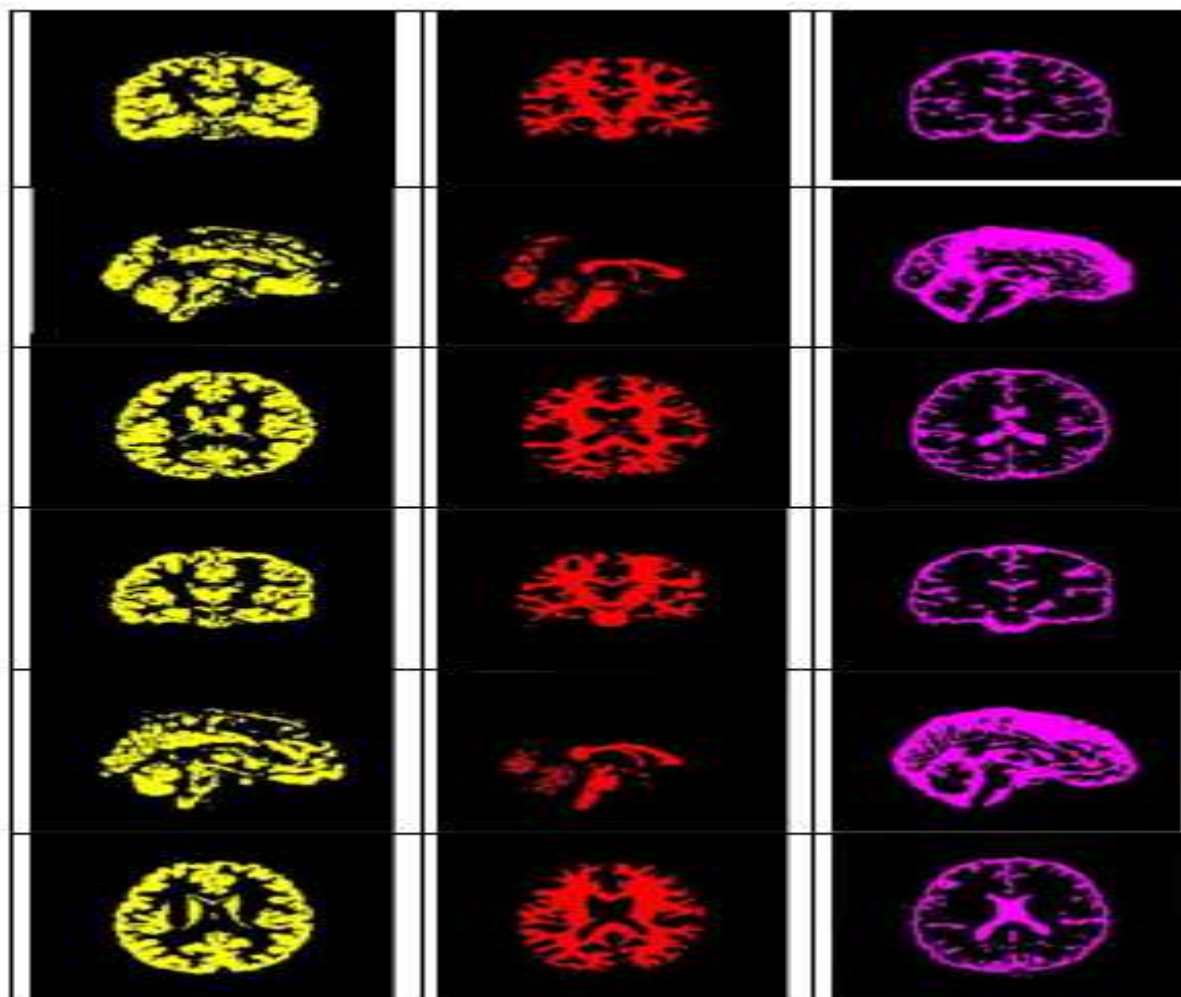
**Figure 3 Pre-processing for the input images**

Figure 3 describes the input MR brain images for ten patients. Figure

(a) refer the input images, Figure 3 (b) denote skull stripped images and Figure 3 (c) denotes the enhanced images







**Figure 4 Segmentation results of K- Means with graph-cut algorithm**

Figure 4 represents the segmentation results of proposed K-Means with graph cut algorithm. Figure 4 (d) denote Grey matter, 4 (e) represents the white matter and 4 (f) represent the CSF region. The outputs are received in 3 anatomical projections such as axial, coronal, and sagittal region like previous

phases. Various cluster center initialization process is executed to prefer the best cluster centers. The proposed segmentation results are compared with K-means with PSO algorithm, MFCM and FFCM algorithms and proved the proposed algorithm provides better segmentation outputs.

**PERFORMANCE MEASURES**

**Table 1 Performance analysis of the proposed algorithm for patient 1**

	AxialRegion			CoronalRegion			SagittalRegion		
	GM	WM	CSF	GM	WM	CSF	GM	WM	CSF
Accuracy	99.42	99.30	99.18	99.40	99.30	99.18	99.37	99.27	99.15
Sensitivity	99.63	99.49	99.47	99.63	99.58	99.47	99.06	99.49	99.42
Specificity	99.20	99.11	98.89	99.17	99.02	98.89	99.15	99.04	98.87
Precision	99.20	99.12	98.90	99.17	99.03	98.90	99.17	99.06	98.89



F-Measure	0.99	0.99	0.99	0.99	0.99	0.99	0.99	0.99	0.99
-----------	------	------	------	------	------	------	------	------	------

**Table 2 Performance analysis for patient 2**

	AxialRegion			CoronalRegion			SagittalRegion		
	GM	WM	CSF	GM	WM	CSF	GM	WM	CSF
Accuracy	99.41	99.30	99.19	99.36	99.28	99.17	99.36	99.28	99.17
Sensitivity	99.62	99.50	99.45	99.57	99.61	99.42	99.63	99.53	99.47
Specificity	99.21	99.10	98.94	99.16	98.95	98.92	99.09	99.06	98.87
Precision	99.22	99.10	98.95	99.16	98.95	98.92	99.09	99.04	98.87
F-Measure	0.99	0.99	0.99	0.99	0.99	0.99	0.99	0.99	0.99

**Table 3 Performance analysis for patient 3**

	AxialRegion			CoronalRegion			SagittalRegion		
	GM	WM	CSF	GM	WM	CSF	GM	WM	CSF
Accuracy	99.32	99.21	99.05	99.27	99.17	99.06	99.25	99.15	99.00
Sensitivity	99.36	99.19	99.02	99.24	99.20	99.11	99.38	99.23	98.92
Specificity	99.31	99.21	99.05	99.28	99.16	99.05	99.21	99.13	99.02
Precision	97.30	994	934	97.19	974	934	994	960	919
F-Measure	0.98	0.98	0.97	0.98	0.97	0.97	0.98	0.97	0.97

**Table 4 Performance analysis for patient 4**

	AxialRegion			CoronalRegion			SagittalRegion		
	GM	WM	CSF	GM	WM	CSF	GM	WM	CSF
Accuracy	99.34	99.24	99.09	99.34	99.20	99.11	99.28	99.17	99.07
Sensitivity	99.56	99.53	99.43	99.55	99.51	99.37	99.54	99.50	99.36
Specificity	99.12	98.95	98.74	99.13	98.89	98.85	99.02	98.84	98.79
Precision	99.13	98.96	98.75	99.13	98.89	98.85	99.03	98.86	98.81
F-Measure	0.99	0.99	0.99	0.99	0.99	0.99	0.99	0.99	0.99

**Table 5 Performance analysis for patient 5**

	AxialRegion			CoronalRegion			SagittalRegion		
	GM	WM	CSF	GM	WM	CSF	GM	WM	CSF
Accuracy	99.42	99.29	99.20	99.39	99.28	99.18	99.34	99.23	99.10
Sensitivity	99.63	99.54	99.53	99.63	99.51	99.45	99.60	99.53	99.36
Specificity	99.21	99.04	98.88	99.14	99.05	98.92	99.12	98.93	98.84
Precision	99.21	99.05	98.89	99.14	99.05	98.93	99.13	98.95	98.86
F-Measure	0.99	0.99	0.99	0.99	0.99	0.99	0.99	0.99	0.99

**Table 6 Performance analysis for patient 6**

	AxialRegion			CoronalRegion			SagittalRegion		
--	-------------	--	--	---------------	--	--	----------------	--	--



	GM	WM	CSF	GM	WM	CSF	GM	WM	CSF
Accuracy	99.06	98.93	98.80	99.02	98.93	98.80	99.03	98.90	98.78
Sensitivity	99.25	99.29	99.16	99.31	99.22	99.21	99.36	99.26	99.15
Specificity	98.87	98.57	98.43	98.74	98.64	98.38	98.71	98.53	98.40
Precision	98.88	98.59	98.45	98.75	98.65	98.40	98.72	98.55	98.44
F-Measure	0.99	0.98	0.98	0.99	0.98	0.98	0.99	0.98	0.98

Table 1 to Table 6 represent the various performance measures of the proposed segmentation method for ten patients. It is estimated in three regions like the axial region, coronal region, and sagittal region for various segmented parts (GM, WM, and CSF). In this analysis, the axial region provides more accuracy as 99.4% in the grey matter than existing works.

Table 7 represents the performance measures of the proposed classification technique in the axial region. Accuracy contains 99.3% for normal cognitive cases, 99.1% for stable MCI cases, 99.3% for progressive MCI cases and 97.7% for Alzheimer's disease cases. Analysis of the proposed method from these results, giving a high accuracy rate and minimum false positive rate in the axial region.

**Table 7 Performance measures of the proposed classification technique in the axial region**

	Normal-cognitive	Stable-MCI	Progressive MCI	Alzheimer's disease
TP	145	140	97	58
TN	302	306	350	382
FP	0	0	0	10
FN	3	4	3	0
Accuracy	93333	91111	93333	97778
Sensitivity	97.973	97.2222	97	98.254
Specificity	100	100	100	97.449
Precision	100	100	100	85.2941
Recall	97.973	97.2222	97	98.332
F-score	0.9898	0.9859	0.9848	0.9206
Jaccardco-efficient	0.9797	0.9722	0.97	0.8529
Missedclassification	0.6667	0.8889	0.6667	2.2222
Performanceindex	0.9933	0.991	0.9933	0.9512
Prevalence	32.8889	32	22.2222	12.8889
False-positivevolume function	0	0	0	0.0255



False-negative volume function	0.0203	0.0278	0.03	0
Genuine acceptance rate	0.9797	0.9722	0.97	1

Table 8 represents the performance measures of the proposed classification technique in the coronal region. Accuracy contains 95.5% for normal cognitive cases, 96% for stable MCI cases, 95.3% for progressive MCI cases and

88% for Alzheimer's disease cases. Analysis of the proposed method from these results, giving a high accuracy rate and minimum false positive rate in the axial region.

**Table 8 Performance measures of the proposed classification technique in the coronal region**

	Normal-cognitive	Stable-MCI	Progressive MCI	Alzheimer disease
TP	145	140	95	15
TN	285	295	334	381
FP	0	0	2	53
FN	20	15	19	1
Accuracy	95.5556	96.6667	95.3333	88
Sensitivity	87.8788	90.3226	83.3333	93.75
Specificity	100	100	99.4048	87.788
Precision	100	100	97.9381	22.0588
Recall	87.8788	90.3226	83.3333	93.75
F-score	0.9355	0.9492	0.9005	0.3571
Jaccardco-efficient	0.8788	0.9032	0.819	0.2174
Missed classification	4.4444	3.3333	4.6667	12
Performance index	0.9535	0.9655	0.9448	0.7249
Prevalence	36.667	34.4444	25.3333	3.5556
False-positive volume function	0	0	0.006	0.1221
False-negative volume function	0.1212	0.0968	0.1667	0.0625
Genuine acceptance rate	0.8788	0.9032	0.8333	0.9375



Table 9 represents the performance measures of the proposed classification technique in the sagittal region. Accuracy contains 90.4% for normal cognitive cases, 92.6% for stable MCI cases, 83.7% for progressive MCI cases and

83.3% for Alzheimer's disease cases. Analysis the proposed method from these results, giving a high accuracy rate and minimum false positive rate in the axial region.

**Table 9 Performance measures of the proposed classification technique in the sagittal region**

	Normal-cognitive	Stable-MCI	Progressive MCI	Alzheimer disease
TP	145	140	44	9
TN	262	277	333	366
FP	0	0	53	59
FN	43	33	20	16
Accuracy	90.4444	92.6667	83.7778	83.3333
Sensitivity	77.1277	80.9249	68.75	36
Specificity	100	100	82694	81176
Precision	100	100	45.3608	13.2353
Recall	77.1277	80.9249	68.75	36
F-score	0.8709	0.8946	0.5466	0.1935
Jaccardco-efficient	0.7713	0.8092	0.3761	0.1071
Missedclassification	9.5556	7.3333	12222	16667
Performanceindex	0.8943	0.9209	0.6425	0.6334
Prevalence	41.7778	38.4444	14.2222	5.5556
False-positivevolume function	0	0	0.1373	0.1388
Falsenegativevolume function	0.2287	0.1908	0.3125	0.64
Genuineacceptance rate	0.7713	0.8092	0.6875	0.36

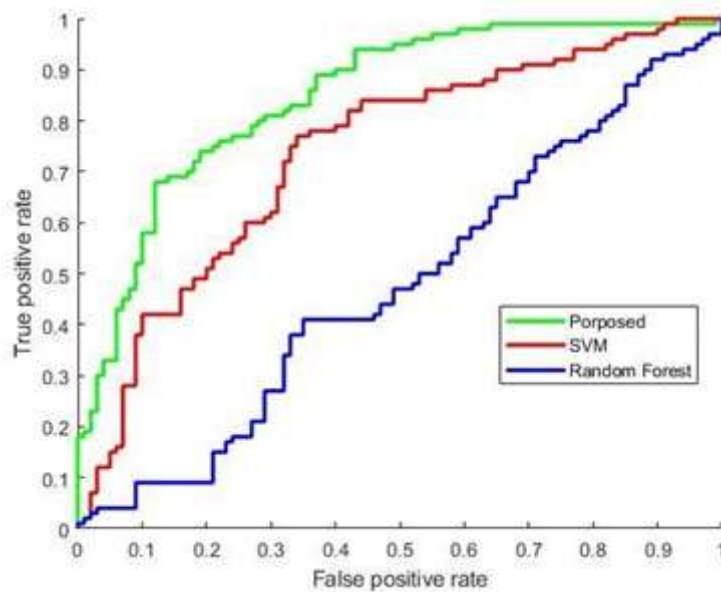
5129

### COMPARATIVE ANALYSIS

In this section, the proposed method results are compared with existing methods such as SVM and Random forest to analyse classification performance.



**Figure 5 ROC curve for proposed game theory classifier**



5130

Figure 5 describes the ROC curve for the proposed classification. This statistical analysis verified that the proposed method has high classification performance compared to SVM and Random forest methods.

**Figure 6 Comparison of proposed method performances with existing methods**

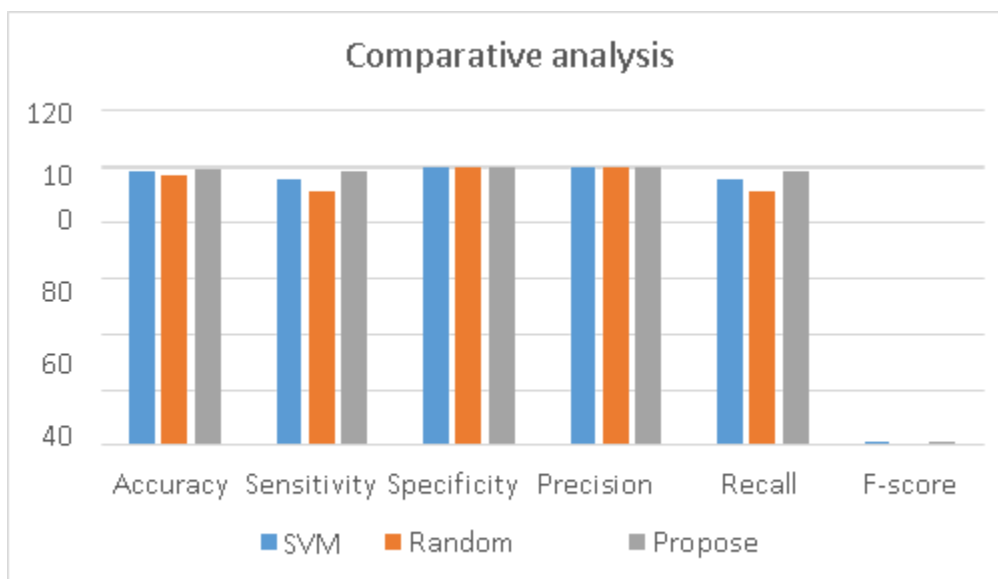


Figure 6 represents the comparison of proposed method performances with existing methods like SVM and Random forest. In this analysis, the accuracy of the SVM method contains 98.4%, the Random forest method had 98%, and the proposed method had high accuracy of 99.3%. From this analysis, the proposed method had high accuracy compared to existing methods.

For performance analysis, we have taken the normal cognitive stage at the axial region. In this research, the work 1 classification provides 94% accuracy, and work 2 provides 96%, work 3 contains 99%, and the final work provides 99.3% in the normal cognitive stage. Likely, other measures provide more performance compared to other works.

5131

**Figure 7 Comparison of proposed works**

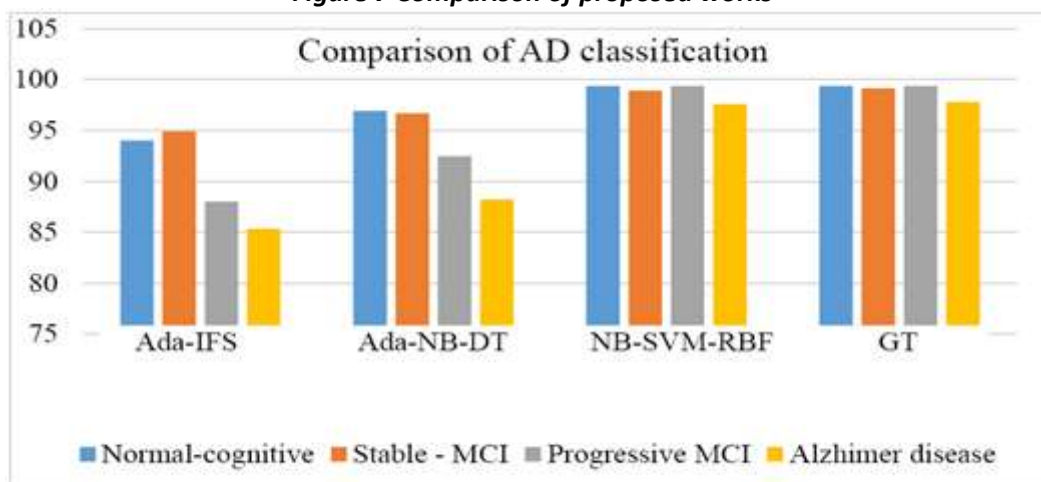


Figure 7 represents the comparison of proposed works of various classification methods. The comparisons are made for normal-cognitive, stable-MCI, progressive MCI and Alzheimer’s disease stages for all the 450

input images. This statistical analysis proves the hybrid clustering with game theory classification provides high accuracy compared to previous works.



## CONCLUSION

This chapter describes the early detection of various stages of Alzheimer's disease. An earlier stage of Alzheimer's disease is evaluated with the help of the novel combinational algorithm. This work used k-means clustering with a graph cut method for segmentation and utilised game theory for classification purpose. In the end, the proposed method of performance analysis was verified with the measures of accuracy, specificity, sensitivity, precision, and recall analysing the effectiveness of the proposed work.

